Prognostic Value and Computer Image Analysis of p53 in Mantle Cell Lymphoma

Yue-Hua Zhang
Sichuan University West China Hospital https://orcid.org/0000-0001-5369-8877
Xiao-Yu Xiang
Sichuan University West China Hospital
Li-Min Gao (hxgaolimin@126.com)
Sichuan University West China Hospital
Wei-Ping Liu
Sichuan University West China Hospital

Research

Keywords: Mantle cell lymphoma, P53, Prognosis, Computer image analysis

Posted Date: October 20th, 2021

DOI: https://doi.org/10.21203/rs.3.rs-970717/v1

Abstract

Background: P53 has different prognostic cut-off values in different mantle cell lymphoma (MCL) studies, and p53 immunohistochemistry (IHC) interpretation is still based on semiquantitative estimation which might be inaccurate. This study aimed to investigate the optimal cut-off value of p53 for predicting prognosis and the possibility of computer image analysis identifying the positive rate of p53 in patients with mantle cell lymphoma (MCL).

Methods: We used QuPath software to determining the p53 positive rate and compared it to the data obtained by manual counting and semiquantitative estimation. Using Youden index and Kaplan-Meier survival curve analysis, we generated survival curves. Chi-squared (χ^2) test was used to compared MCL cell morphology with p53. Spearman rank correlation test and Bland-Altman analysis were used to compared manual counting, computer image analysis and semiquantitative estimation.

Results: The optimal cut-off value of p53 for predicting prognosis was 20% in MCL patients. Patients with p53 ≥ 20% had a significantly worse overall survival (OS) compared to p53 < 20% (P < 0.0001). MCL patients with blastoid/pleomorphic variant cell morphology had more p53 ≥ 20% than classical type (P < 0.0001). And a strong correlation between computer image analysis and manual counting p53 in the same areas in MCL patients (spearman's rho = 0.966, P < 0.0001).

Conclusions: MCL patients with p53 ≥ 20% have a shorter OS, and a blastoid/pleomorphic variant tendency. Computer image analysis could reflect the actual positive rate of p53 and is a more attractive alternative than semiquantitative estimation in MCL.

Background

Mantle cell lymphoma (MCL) is an aggressive B-cell non-Hodgkin lymphoma (NHL) and comprises about 3–10% of NHL [1–3]. MCL clinical prognoses are heterogeneous, and risk stratification is based on the clinical indexes comprising the Mantle Cell Lymphoma Prognostic Index (MIPI) and a combined biological MIPI, including Ki67 [4–6]. However, risk stratification might be further improved by biological markers, such as p53. P53 protein expression might serve as an alternative marker for *TP53* gene mutations [7–9] and has been confirmed to be of prognostic value independent of the biological MIPI score in a few MCL studies [7, 10–12]. However, p53 has different prognostic cut-off values in different studies, which is still controversial. Furthermore, p53 immunohistochemistry (IHC) interpretation is still based on semiquantitative estimation,which is inaccurate because of more considerable inter-observer variability. Therefore, practical and efficient means for precisely interpret the positive rate of p53 with less inter-observer variability would be of great attraction in MCL.

In the present study, we aimed to investigate the prognostic cut-off value of p53 in MCL. Meanwhile, we applied computer image analysis software to calculate p53 in MCL patients and compared the data to the results obtained from manual counting and semiquantitative estimation in routine clinical diagnostics.

Methods

Patients

A cohort of 65 MCL specimens was obtained from the Department of Pathology, West China Hospital of Sichuan University from 2014 to 2021. All cases were newly diagnosed and reviewed by trained pathologists according to the 2016 World Health Organization (WHO) classification for tumours of hematopoietic and lymphoid tissues [13]. Anonymous data regarding the gender, age, Ann Arbor stage, tumour tissue type, tumour cell morphology, and survival time were obtained retrospectively from the patients' medical records and telephone follow-ups. All patients were followed up from the date of diagnosis to July 31, 2021. The Medical Ethics Committee approved this study of West China Hospital of Sichuan University (The registration number: WCH2021-00333). All recruited patients gave written informed consent following the Declaration of Helsinki.

Immunohistochemistry Staining Of P53

The EliVision method was used for immunohistochemistry (IHC) staining of p53 [14]. Briefly, the paraffin blocks were cut into 4μm sections, pretreated in ethylenediaminetetraacetic acid (EDTA) buffer at pH 9.0 for 20 minutes and incubated with p53 at dilution 1:200 (clone DO-7; MXB Biotechnologies, Fuzhou, China) and 3,3’-diaminobenzidine (DAB) chromogen, finally counterstained with hematoxylin and rinsed with deionized water. The expression of p53 was detected in the tumour cell nucleus. Each slide was scanned by the Hamamatsu Digital Slide Scanner NanoZoomer 2.0-HT C9600-13.

Manual counting, computer image analysis and semiquantitative estimation of p53-positive cells

Manual counting and computer image analysis of each image used QuPath software (version 0.1.2) [15, 16]. Representative regions from each slide were annotated by an experienced pathologist and a Ph.D. student. Regions involving a high density of lymphoma cells were chosen, avoiding hotspot areas. Images were extracted from the typical region, and identical areas were selected for random manual counting and computer image analysis. When manually counting the selected images, at least 1000 tumour cells were acquired in each slide. Hematopathologists chosen the representative areas and obtained Semiquantitatively estimated p53.

Statistical analysis

Overall survival (OS) was defined as the number of days from diagnosis to the date of death or final follow-up. The sensitivity and specificity of p53 were tested by assessing the area under the ROC curve (AUC). Further, the Youden index and optimal cut-off value were calculated using the DeLong test [17]. Survival curves were generated using the Kaplan-Meier survival analysis method, and the log-rank test was used to examine differences in OS. Comparisons of cell morphology and p53 were conducted using the Chi-squared (χ^2) test. The spearman rank correlation test calculated the correlation between manual counting, computer image analysis, and semiquantitative estimation. Bland-Altman analysis was used for comparison of manual counting, computer image analysis and semiquantitative estimation [18, 19]. Statistical analyses were performed using the MedCalc, 20.009 software (MedCalc Software Ltd), and $P < 0.05$ was considered statistically significant.

Results

Patient characteristics

The cohort included 65 MCL patients. The male to female rate was 2.61:1, and the median age was 63. Thirty-eight (58%) patients were at Ann Arbor stage □-□ and 27 (42%) at stage □-□. Among these patients, 43 (66%) tumour tissue specimens were derived from lymph nodes, and others included the gastrointestinal tract, tonsil, nasopharynx, bone marrow, etc. The tumour cell morphology of 36 (55%) patients was the classical type, and 29 (45%) patients were blastoid/pleomorphic variant. Follow-up data were obtained for all 65 patients, and 51 (78%) patients died with MCL (Table1).

Table 1
Clinical and pathological features of MCL patients.

Category		n	%
Gender	Male	47	72
	Female	18	28
Age [median (range)]		63 (38-84)	NA
Ann Arbor stage	□-□	38	58
	□-□	27	42
Tumour tissue type	Lymph node	43	66
	Gastrointestinal tract	9	14
	Tonsil	5	8
	Nasopharynx	2	3
	Bone marrow	2	3
	Others	4	6
Cell morphology	Classical type	36	55
	Blastoid/Pleomorphic variant	29	45
Survival state	Survival	14	22
	Dead	51	78
MCL, mantle cell lymphoma; NA, Not Applicable.			

Manual counting, computer image analysis and semiquantitative estimation of p53: correlation with survival and cell morphology

Figure 1 showed images based on manual counting (Fig. 1A) and computer image analysis (Fig. 1B) on the identical image from a representative region. The median p53 assessed by manual counting at least 1000 tumour cells was 43.1%, and the mean was 45.0% (range 0-100%). The median p53 calculated by computer image analysis of the same areas by manual counting was 53.3%, with a mean of 48.2% (range 0.1-100%). And the p53 acquired by semiquantitative estimation displayed a median of 40% and a mean of 39.4% (range 0-100%).

Manual counting, computer image analysis and semiquantitative estimation of p53 can predict OS. Each of these methods showed an AUC > 0.85 on ROC curves (P < 0.0001; Fig. 2, Table 2. The optimal p53 cut-off for predicting OS are: manual counting, cut-off value, 16.20%, sensitivity, 80.39%, specificity, 100%; computer image analysis, cut-off value, 17.66%, sensitivity, 74.51%, specificity, 100%; semiquantitative estimation, cut-off value, 5.00%, sensitivity, 76.47%, specificity, 92.86% (Table 2). As manual counting and computer image analysis are more precise than semiquantitative estimation, we used the approximate value of manual counting and computer image analysis, 20%, as the cut-off value of p53 for subsequent analysis.

Table 2
Diagnostic performance of p53 measured by different methods.

	AUC (95% CI)	P	Youden index	Optimal cut-off	Sensitivity (95% CI)	Specificity (95% CI)
Manual counting	0.873 (0.767 - 0.943)	<0.0001	0.8039	16.20%	80.39% (66.9% - 90.2%)	100% (76.8% - 100%)
Computer image analysis	0.853 (0.743 - 0.929)	<0.0001	0.7451	17.66%	74.51% (60.4% - 85.7%)	100% (76.8% - 100%)
Semiquantitative estimation	0.856 (0.747 - 0.931)	<0.0001	0.6933	5.00%	76.47% (62.5% - 87.2%)	92.86% (66.1% - 99.8%)

AUC, area under curve; CI, confidence interval.

To assess the prognosis of these three methods, we performed survival analysis. Kaplan-Meier survival curve analysis showed that patients with p53 < 20% have a significantly longer OS than patients with p53 ≥ 20% (P < 0.0001, Fig. 3A-C). Meanwhile, patients with blastoid MCL had shorter OS than those with classical MCL (P < 0.0001, Fig

3D). And blastoid/pleomorphic variant MCL patients had more p53 ≥ 20% as compared to classical type (P < 0.0001, Table 3).

Table 3
Correlation analysis of p53 and cell morphology.

Cell morphology	P53 by manual counting				P53 by computer image analysis				P53 by semiquantitative estimation			
	< 20%	≥ 20%	χ^2	P	< 20%	≥ 20%	χ^2	P	< 20%	≥ 20%	χ^2	P
Classical type	23	13	21.703	< 0.0001	23	13	21.703	< 0.0001	26	10	27.523	< 0.0001
Blastoid/Pleomorphic variant	2	27			2	27			2	27		

CI, confidence interval.

Correlation between manual counting, computer image analysis and semiquantitative estimation

There was a strong correlation between manual counting and computer image analysis of p53 in the identical areas (spearman's rho = 0.966, P < 0.0001, Fig. 4A). There was a significant correlation between manual counting and semiquantitative estimation (spearman's rho = 0.938, P < 0.0001, Fig. 4B), albeit weaker than the correlation between manual counting and computer image analysis. Moreover, we found a significant correlation between semiquantitative estimation and computer image analysis (spearman's rho = 0.898, P < 0.001, Fig. 4C).

Bland-Altman plots comparing manual counting with computer image analysis of identical areas revealed a tendency toward a higher evaluation of p53 by computer image analysis (Fig. 4D), and comparing manual counting p53 with semiquantitative estimation revealed a tendency towards a lower evaluation of p53 by semiquantitative estimation (Fig. 4E). We also used the Bland-Altman plot to compare computer image analysis with the semiquantitative estimation of identical areas. The result revealed a tendency toward a lower evaluation of p53 by semiquantitative estimation (Fig. 4F).

Discussion

In this study, we demonstrated that 20% could be used as the optimal cut-off value for judging the prognosis of MCL. MCL patients with p53 ≥ 20% had a shorter OS than p53 < 20%. In addition, patients with blastoid/pleomorphic variant MCL tended to have p53 ≥ 20%. We also verified that the possibility of computer image analysis software to count p53 in patients with MCL.

IHC staining for p53 is a promising tool for the predictive purpose, as it serves as an alternative marker for *TP53* mutation and 17p deletion [7–9, 20]. In MCL, the prognostic significance of p53 immunohistochemical expression has been studied (Table 4). Rodrigues et al. also used manual counting and computer image analysis for p53 immunohistochemical counting and prognosis analysis [7]. They defined 30% as the prognostic cut-off value of p53, which is based on previous publication [11] and clinical routine at Lund University Hospital. Meanwhile, the prognostic cut-off values of p53 in MCL in other studies are controversial, ranging from 1%-50%, and the criteria for defining these cut-off values are unclear [10–12, 21]. We used manual counting and computer image analysis to count the positive rate of p53 and calculated the cut-off values for predicting OS with the optimal specificity and sensitivity through the Youden index. Manual counting was 16.20%, computer image analysis was 17.66%. To facilitate clinical application, we used 20% as the cut-off value of p53 for survival analysis, and the results revealed that MCL patients with p53 ≥ 20% had a worse prognosis than those p53 < 20%. In addition, we also found that p53 ≥ 20% was associated with blastoid morphology, which is consistent with previous studies [12, 20, 22].

Table 4
Summary of p53 cut-off values and prognostic significance of MCL cases from kinds of literature and our study.

Author	Cases	P53 immunohistochemistry		
		Cut off value	Positive rate	Prognostic significance
Our study	65	20%	40/65	Worse
Aukema SM [10]	365	50%	16/365	Worse
Rodrigues JM [7]	317	30%	42/317	Worse
Nordström L [11]	93	30%	10/93	Worse
Choe JY [12]	62	30%	-	Worse
Abrisqueta P [21]	40	1%	5/40	Worse
-, not mention.				

Manual counting is very time-consuming and probably not be applicable in a clinical routine test. Thus, we compared three methods of p53 counting to define a simple and accurate method. We confirmed that p53 by computer image analysis was more precise for prognosis prediction and had a stronger correlation with manual counting than semiquantitative estimation. Computer image analysis of p53 could count larger tumour regions than manual counting, making it more representative to access the percentage of p53-positive cells within the tumour. Additionally, computer image analysis is faster than manual counting and creates repeatable results for retrospection.

The computer image analysis revealed a tendency towards slightly higher estimates of p53 compared to manual counting. Further analysis reasons that contributed to the overestimation of p53 may include positively staining background cells miscalled as tumour cells, debris miscalled as positive staining [23]. Therefore, computer image analysis would possibly benefit from strict quality control of the IHC staining method.

The limitation of computer image analysis is the inability to distinguish between different cell types such as normal cells and tumour cells [24]. Consequently, representative regions of lymphoma must be chosen carefully by pathologists. While the pathologists choose the representative region of lymphoma, this would not be a weakness in MCL because the reactive cells number is low in MCL [25].

Conclusions

We demonstrated that MCL patients with p53 ≥ 20% had a shorter OS, and a blastoid/pleomorphic variant tendency. Furthermore, computer image analysis of p53 is more precise than semiquantitative estimation and can be applied to the interpretation of p53 IHC staining in patients with MCL.

Abbreviations

MCL

mantle cell lymphoma
OS
overall survival
χ^2
chi-squared
NHL
non-Hodgkin lymphoma
MIPI
Mantle Cell Lymphoma Prognostic Index
IHC
immunohistochemistry
WHO
World Health Organization
EDTA
ethylenediaminetetraacetic acid
DAB
diaminobenzidine
AUC
area under the ROC curve
NA
Not Applicable
CI, confidence interval.

Declarations

Ethics approval and consent to participate

The present study was approved by the Institutional Review Board of West China Hospital of Sichuan University (WCH2021-00333). All subjects signed informed consent forms before participating.

Consent for publication

All subjects signed informed consent forms before participating.

Availability of data and materials

The datasets used and/or analyzed during the current study are available from the corresponding author on reasonable request.

Competing interests

The authors declare that they have no competing interests related to the present study.

Funding

This study was supported by the national natural science foundation of China (81900197) and Science and Technology Program of Sichuan Province (2020YJ0104).

Authors' contributions

YHZ, LMG and WPL contributed to the conceptual design of the study. YHZ and XYX were involved in data acquisition. YHZ and LMG were involved in data analysis and interpretation. YHZ and LMG were involved in writing and editing the manuscript. YHZ, XYX, LMG and WPL reviewed the manuscript. This study was supervised by WPL and LMG.

Acknowledgements

Not applicable.

References

1. Jain P, Wang M. Mantle cell lymphoma: 2019 update on the diagnosis, pathogenesis, prognostication, and management. Am J Hematol. 2019;94(6):710–25. doi:10.1002/ajh.25487.
2. Hermine O, Hoster E, Walewski J, Bosly A, Stilgenbauer S, Thieblemont C, et al. Addition of high-dose cytarabine to immunochemotherapy before autologous stem-cell transplantation in patients aged 65 years or younger with mantle cell lymphoma (MCL Younger): a randomised, open-label, phase 3 trial of the European Mantle Cell Lymphoma Network. Lancet. 2016;388(10044):565–75. doi:10.1016/s0140-6736(16)00739-x.
3. LI X-q LI, G-d GAO, Z-f. ZHOU X-g, ZHU X-z. Distribution pattern of lymphoma subtypes in China: A nationwide multicenter study of 10002 cases. Journal of Diagnostics Concepts Practice. 2012;11(02):111–5.
4. Hoster E, Dreyling M, Klapper W, Gisselbrecht C, van Hoof A, Kluin-Nelemans HC, et al. A new prognostic index (MIPI) for patients with advanced-stage mantle cell lymphoma. Blood. 2008;111(2):558–65. doi:10.1182/blood-2007-06-095331.
5. Hoster E, Rosenwald A, Berger F, Bernd HW, Hartmann S, Loddenkemper C, et al. Prognostic Value of Ki-67 Index, Cytology, and Growth Pattern in Mantle-Cell Lymphoma: Results From Randomized Trials of the European Mantle Cell Lymphoma Network. Journal of clinical oncology: official journal of the American Society of Clinical Oncology. 2016;34(12):1386–94. doi:10.1200/jco.2015.63.8387.
6. Dreyling M, Campo E, Hermine O, Jerkeman M, Le Gouill S, Rule S, et al. Newly diagnosed and relapsed mantle cell lymphoma: ESMO Clinical Practice Guidelines for diagnosis, treatment and follow-up. Annals of oncology: official journal of the European Society for Medical Oncology. 2017;28(suppl_4):iv62–71. doi:10.1093/annonc/mdx223.
7. Rodrigues JM, Hassan M, Freiburghaus C, Eskelund CW, Geisler C, Räty R, et al. p53 is associated with high-risk and pinpoints TP53 missense mutations in mantle cell lymphoma. Br J Haematol. 2020;191(5):796–805. doi:10.1111/bjh.17023.
8. Stefancikova L, Moulis M, Fabian P, Ravcukova B, Vasova I, Muzik J, et al. Loss of the p53 tumor suppressor activity is associated with negative prognosis of mantle cell lymphoma. Int J Oncol. 2010;36(3):699–706. doi:10.3892/ijo_00000545.
9. Jing C, Zheng Y, Feng Y, Cao X, Xu C. Prognostic significance of p53, Sox11, and Pax5 co-expression in mantle cell lymphoma. Scientific reports. 2021;11(1):11896. doi:10.1038/s41598-021-91433-7.
10. Aukema SM, Hoster E, Rosenwald A, Canoni D, Delfau-Larue MH, Rymkiewicz G, et al. Expression of TP53 is associated with the outcome of MCL independent of MIPI and Ki-67 in trials of the European MCL Network. Blood. 2018;131(4):417–20. doi:10.1182/blood-2017-07-797019.
11. Nordström L, Sernbo S, Eden P, Grønbaek K, Kolstad A, Räty R, et al. SOX11 and TP53 add prognostic information to MIPI in a homogenously treated cohort of mantle cell lymphoma–a Nordic Lymphoma Group study. Br J Haematol. 2014;166(1):98–108. doi:10.1111/bjh.12854.
12. Choe JY, Yun JY, Na HY, Huh J, Shin SJ, Kim HJ, et al. MYC overexpression correlates with MYC amplification or translocation, and is associated with poor prognosis in mantle cell lymphoma. Histopathology. 2016;68(3):442–9. doi:10.1111/his.12760.
13. Swerdlow SH, Campo E, Harris NL, Jaffe ES, Pileri SA. WHO Classification of Tumours of Haematopoietic and Lymphoid Tissues. Revised 4th Edition. Lyon, France: IARC press; 2017.
14. Kämmerer U, Kapp M, Gassel AM, Richter T, Tank C, Dietl J, et al. A new rapid immunohistochemical staining technique using the EnVision antibody complex. The journal of histochemistry cytochemistry: official journal of the Histochemistry Society. 2001;49(5):623–30. doi:10.1177/002215540104900509.
15. Bankhead P, Loughrey MB, Fernández JA, Dombrowski Y, McArt DG, Dunne PD, et al. QuPath: Open source software for digital pathology image analysis. Scientific reports. 2017;7(1):16878. doi:10.1038/s41598-017-17204-5.
16. Paulik R, Micsik T, Kiszler G, Kaszál P, Székely J, Paulik N, et al. An optimized image analysis algorithm for detecting nuclear signals in digital whole slides for histopathology. Cytometry Part A: the journal of the International Society for Analytical Cytology. 2017;91(6):595–608. doi:10.1002/cyto.a.23124.
17. DeLong ER, DeLong DM, Clarke-Pearson DL. Comparing the areas under two or more correlated receiver operating characteristic curves: a nonparametric approach. Biometrics. 1988;44(3):837–45.
18. Bland JM, Altman DG. Measuring agreement in method comparison studies. Stat Methods Med Res. 1999;8(2):135–60. doi:10.1177/096228029900800204.
19. Bland JM, Altman DG. Statistical methods for assessing agreement between two methods of clinical measurement. Lancet. 1986;1(8476):307–10.
20. Slotta-Huspenina J, Koch I, de Leval L, Keller G, Klier M, Bink K, et al. The impact of cyclin D1 mRNA isoforms, morphology and p53 in mantle cell lymphoma: p53 alterations and blastoid morphology are strong predictors of a high proliferation index. Haematologica. 2012;97(9):1422–30. doi:10.3324/haematol.2011.055715.

21. Abrisqueta P, Scott DW, Slack GW, Steidl C, Mottok A, Gascoyne RD, et al. Observation as the initial management strategy in patients with mantle cell lymphoma. Annals of oncology: official journal of the European Society for Medical Oncology. 2017;28(10):2489–95. doi:10.1093/annonc/mdx333.
22. Kimura Y, Sato K, Arakawa F, Karube K, Nomura Y, Shimizu K, et al. Mantle cell lymphoma shows three morphological evolutions of classical, intermediate, and aggressive forms, which occur in parallel with increased labeling index of cyclin D1 and Ki-67. Cancer Sci. 2010;101(3):806–14. doi:10.1111/j.1349-7006.2009.01433.x.
23. Naso JR, Povshedna T, Wang G, Banyi N, MacAulay C, Ionescu DN, et al. Automated PD-L1 Scoring for Non-Small Cell Lung Carcinoma Using Open-Source Software. Pathology oncology research: POR. 2021;27:609717. doi:10.3389/pore.2021.609717.
24. Duan K, Jang GH, Grant RC, Wilson JM, Notta F, O'Kane GM, et al. The value of GATA6 immunohistochemistry and computer-assisted diagnosis to predict clinical outcome in advanced pancreatic cancer. Scientific reports. 2021;11(1):14951. doi:10.1038/s41598-021-94544-3.
25. Klapper W. Histopathology of mantle cell lymphoma. Semin Hematol. 2011;48(3):148–54. doi:10.1053/j.seminhematol.2011.03.006.

Figures

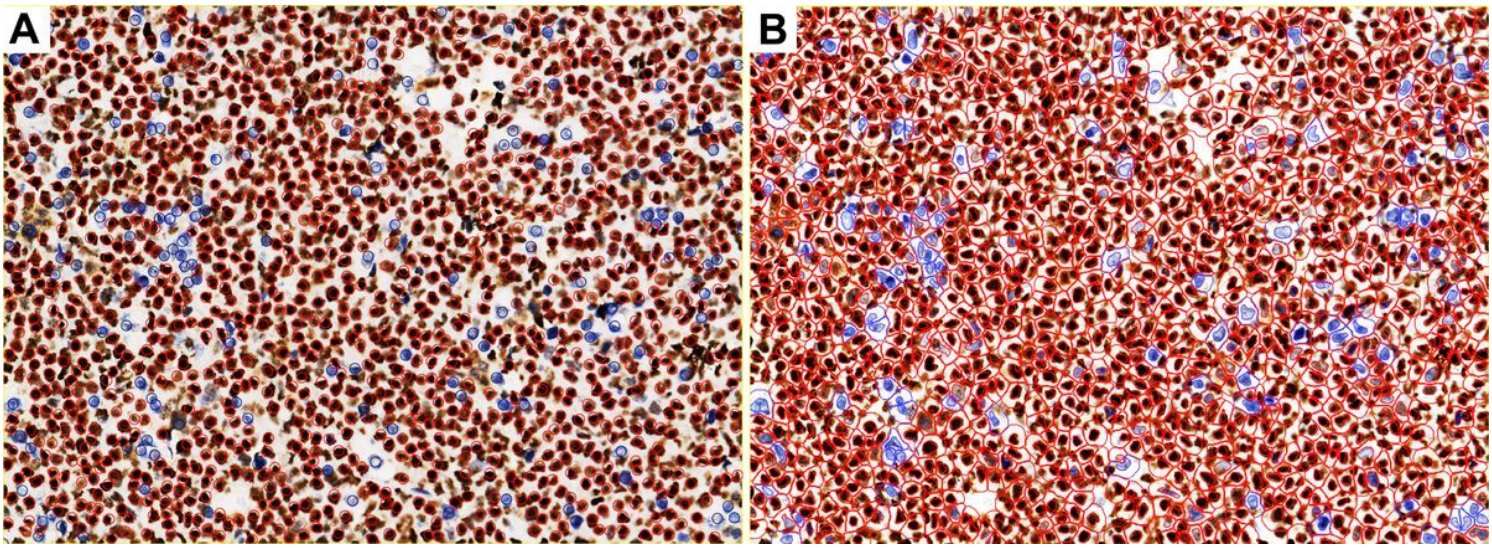

Figure 1

Image analysis of p53-positive tumour cells in identical areas chose a specific region at random in one case. (A) image-based manual counting, positively stained (brown) and negative nuclei (blue) marked red and blue circles. (B) image-based computer image analysis, positively stained (brown) and negative nuclei (blue) marked red and blue irregular circles.

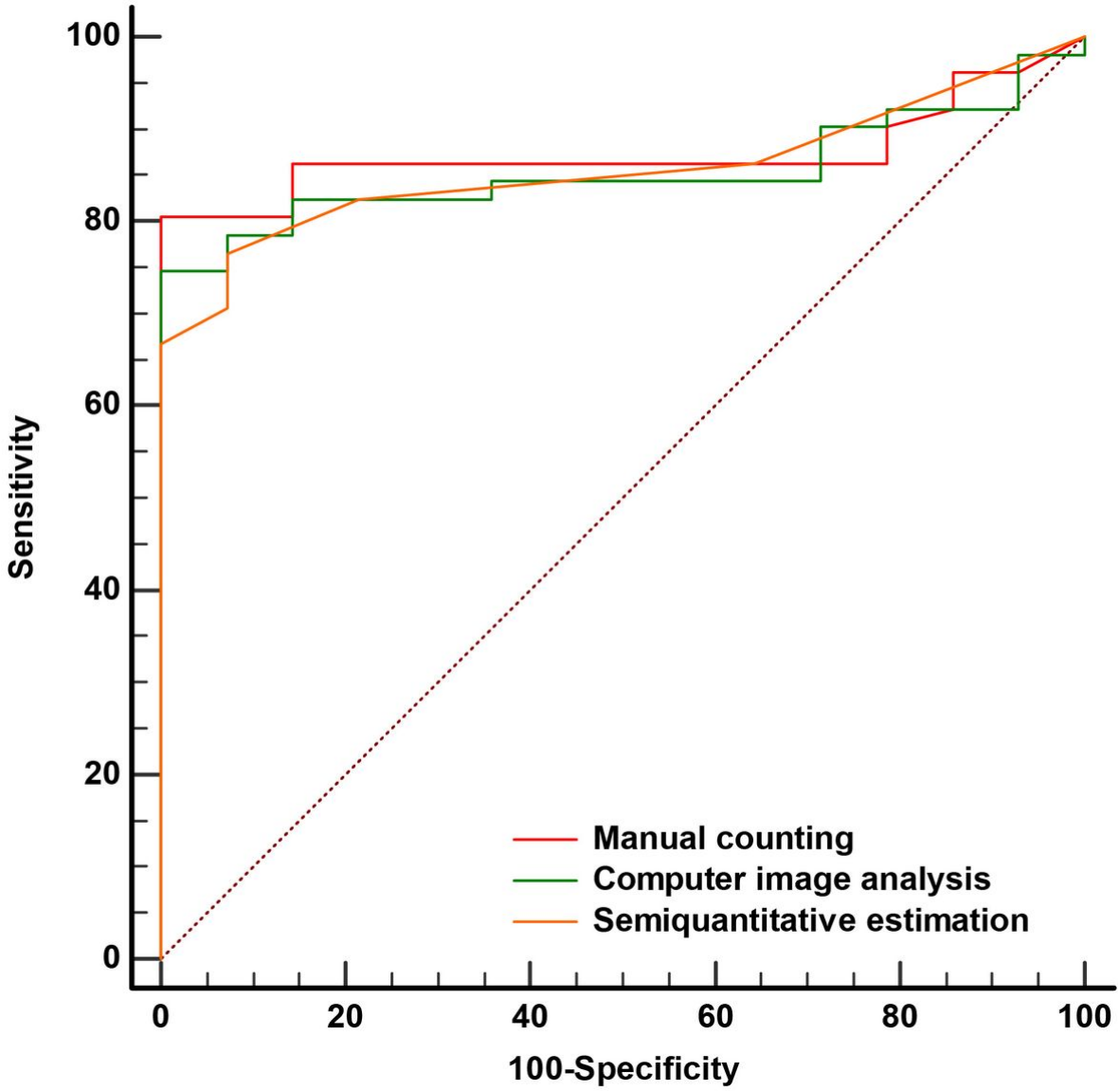

Figure 2

Discriminatory power for p53 predicting overall survival (OS).

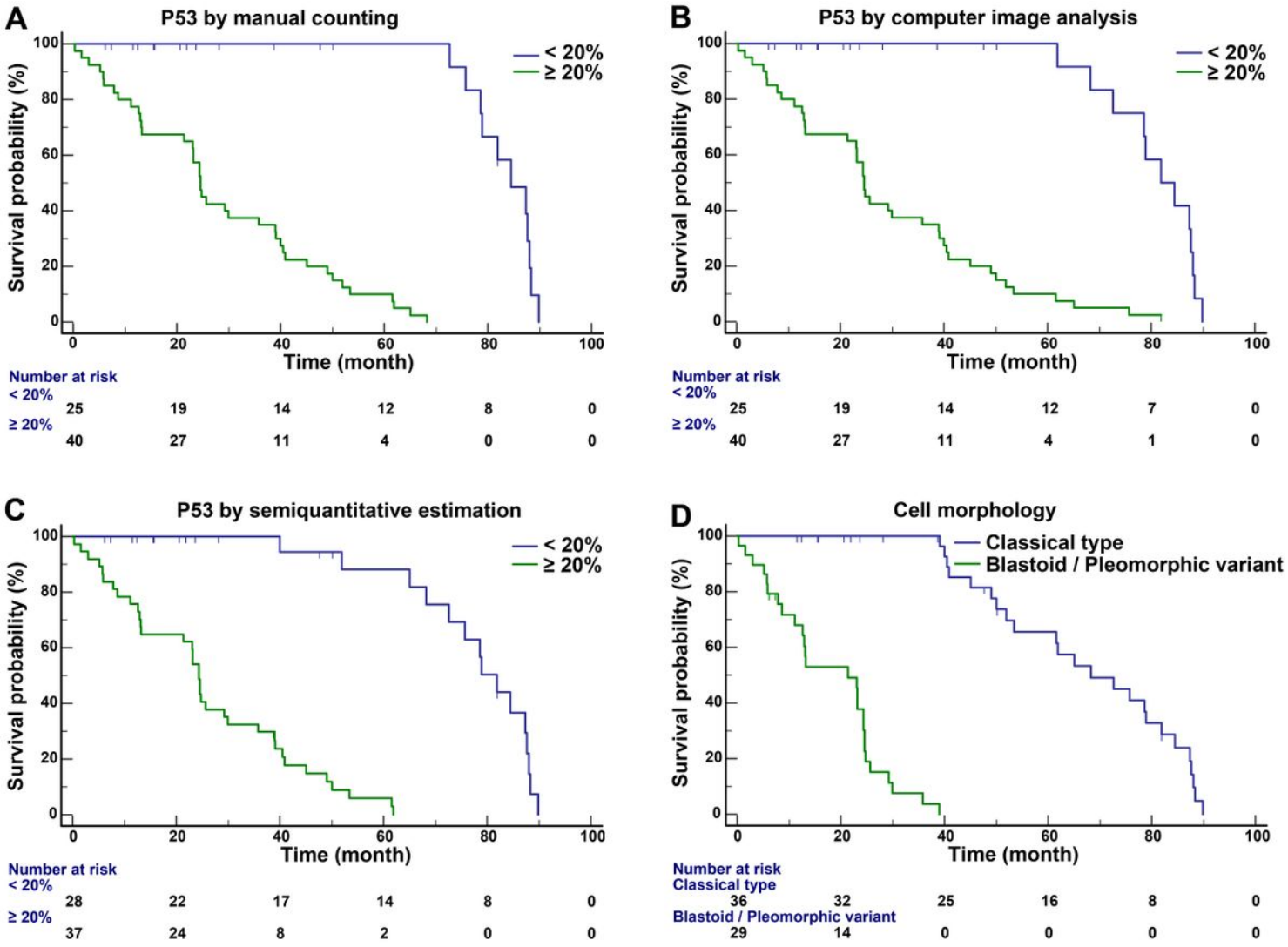

Figure 3

Overall survival (OS) according to (A) p53 by manual counting, (B) p53 by computer image analysis, (C) p53 by semiquantitative estimation, (D) classical type versus blastoid variant cell morphology.

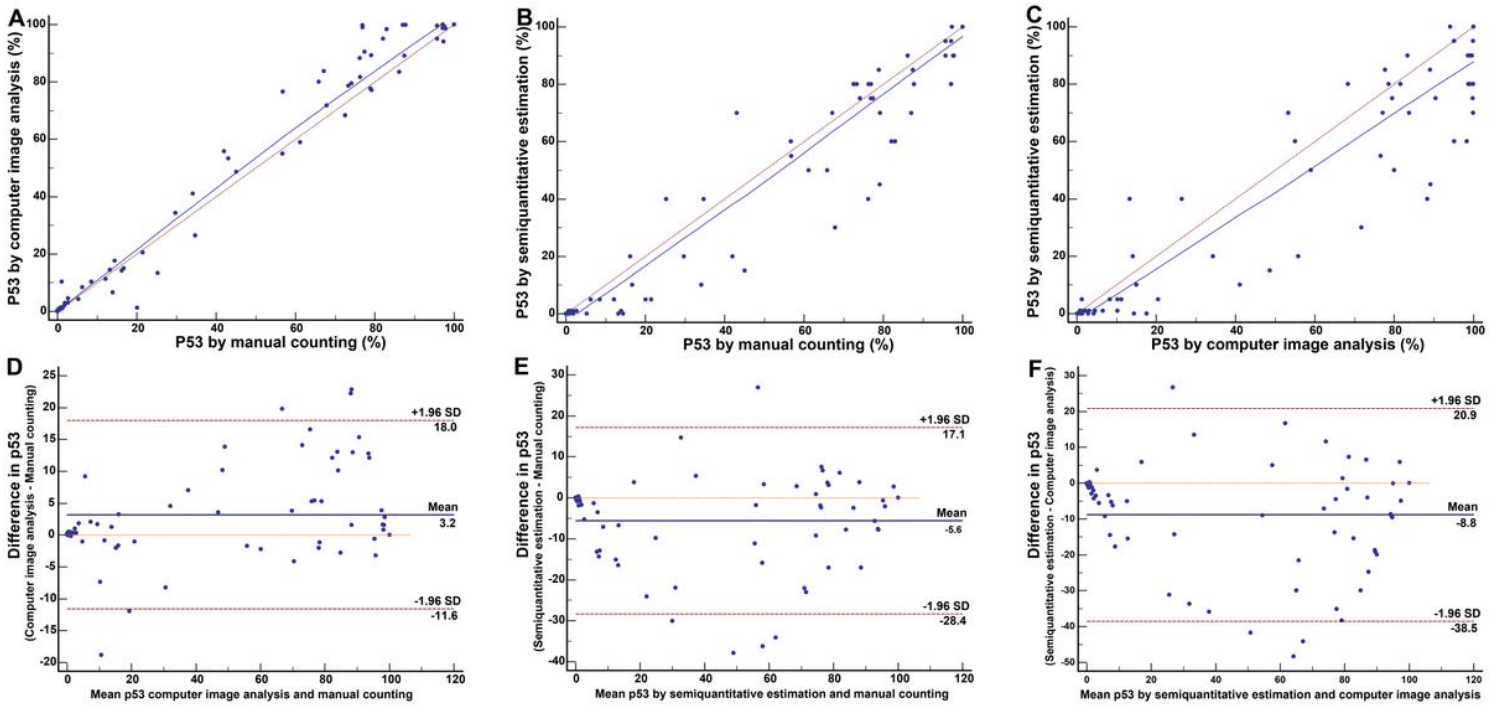

Figure 4

Correlation between (A) computer image analysis and manual counting of p53, (B) semiquantitative estimation and manual counting of p53, and (C) semiquantitative estimation and computer image analysis of p53 in identical areas. Bland-Altman plots comparing p53 by (D) computer image analysis with manual counting, (E) semiquantitative estimation with manual counting, and (F) semiquantitative estimation with computer image analysis of identical areas.

Supplementary Files

This is a list of supplementary files associated with this preprint. Click to download.

- Graphicalabstract.jpg